ISTITUTO NAZIONALE DI FISICA NUCLEARE
Laboratori Nazionali di Frascati

LNF-83/93

E. Iarocci: PLASTIC STREAMER TUBES AND THEIR APPLICATIONS IN HIGH ENERGY PHYSICS

Estratto da:
Nuclear Instr. and Meth. 217, 30 (1983)

Servizio Documentazione
dei Laboratori Nazionali di Frascati
Cas. Postale 13 - Frascati (Roma)

Nuclear Instruments and Methods 217 (1983) 30–42
North-Holland Publishing Company

PLASTIC STREAMER TUBES AND THEIR APPLICATIONS IN HIGH ENERGY PHYSICS

E. IAROCCI
Laboratori Nazionali INFN, Frascati, Italy

A review of the basic performance and technology of plastic streamer tubes is presented, together with their applications and developments essentially in the field of digital tracking calorimetry, based on either digital patterns or charge readout, or both, with different pick-up electrode arrangements.

1. Introduction

The development of plastic streamer tubes started in Frascati in 1976. The first prototype was a plexiglass tube with a resistive graphite coating on the inside and a helix wound around the outside, to localize tracks along the tube, by the delayed helix pulse, picked-up through the transparent resistive cathode. It is easy to understand that plastic tubes with resistive cathode could be easily combined with any kind of pick-up electrodes simply placed around. The first tubes were 2–3 cm in diameter, with 100 μm thick wires mounted in the center. They were operated in the limited streamer mode, by using the standard argon + isobutane (70 + 30) drift chamber mixture [1]. A small plastic streamer tube detector (200 tubes) with external strips placed across the tube layers, was operated in 1978 as the inner detector in the $\gamma\gamma 2$ experiment at Adone, the Frascati storage ring [2].

It must be noticed that streamer tubes were used in an experiment before the exact nature of their operation mode was clearly understood. After occasional observations by many authors which can be tracked back to 1970 [3], the first systematic study of the streamer mode, characterized by large signals with thick anode wires, was performed by Charpak et al. (1975) [4]. At that time it was interpreted as a limited Geiger mode, i.e. a discharge surrounding the wire and propagating along it, with natural self-quenching within ~ 1 cm. Later on (1977) the streamer nature of the discharge was established by Charpak et al. [5] and Fisher et al. [6]: it was observed that the centroid of charge generated by the process was definitely outside the center of the wire, suggesting a propagation from the wire towards the cathode. Subsequently there was direct visual assessment by pictures of the self-quenching streamer nature of the process by Alekseev et al. [7]. Recently (1981) Atac et al. [8] succeeded, by making use of image intensifiers, in obtaining detailed pictures of single streamers, which appeared as very thin (~ 200 μm) filamentary discharge channels, starting from the wire and propagating along a few millimeters towards the cathode.

The work started in Frascati on the streamer mode, in conjunction with the development of the resistive cathode idea, established the basic streamer mode properties, like the noiseless and uncritical operation, and, most important, the basic conditions to achieve them [9].

The development of resistive cathode devices induced the use of unconventional materials. The simplicity of the tube device, with thick wires and the uncritical streamer operation, and also the simplicity of the external pick-ups, which did not require the precision and cleanliness of cathode electrodes, favoured the exploitation of using inexpensive materials, not common with the standards of wire chambers.

In 1977 at Orsay the construction of a plastic streamer tube system was started (several thousands), with a helical delay line readout, for the photon and muon detectors of DM2 [10], which is presently running. Both the $\gamma\gamma 2$ and DM2 tubes were 2 cm in cross section: it took a couple of years to understand how to work with smaller tubes (1978) [9], which at first looked to be critical. The first large scale application of small streamer tubes was the implementation of the CHARM detector with 20000 1 cm^2 aluminum tubes (1979) [11]. In 1980 a Frascati–Milano–Torino–CERN collaboration started the construction of the Mont Blanc proton decay detector, entirely based on the use of plastic streamer tubes with x–y strip readout [12]. On this occasion the problem of the engineering of a large system was faced: ~ 50000 tubes, 100000 strips, 3.5 m long, for a total pick-up area of 3400 m^2 [13]. On this occasion one took advantage of the favourable technological properties of thermoplastic materials in automated production lines for manufacturing PST (plastic streamer tubes) in a quick and modular way. The Mont Blanc tubes have now been turned on for one year and they perform in accordance with the most optimistic previsions. In this

0167-5087/83/0000–0000/$03.00

experiment the tubes fit into a simple cubic sandwich of 3.5 m length, with pick-up strips connected to a digital readout. This digital tracking calorimeter is arranged in such a way in order to detect particles as soft as 200 MeV muons, in an extremely low rate environment, dominated by the natural rdioactivity [14].

However, this particular PST device can easily fit into many different experimental lay-outs, fulfilling a variety of detector tasks.

The tube-strip system with digital readout is useful as a tracking device (3 mm spatial accuracy), and allows straightforward calorimetry by hit counting, limited to relatively low energy, but with a resolution close to the best values achievable in sampling calorimetry.

Although, in principle, two factors impose a limitation on the rate capability, i.e. the high current mode and the resistive cathode, in practice, in high energy physics applications, experimental situations are unlikely to occur where these factors impose a problem. Their maximum sustainable particle rate, with negligible efficiency loss, is around $10^6/s \cdot m^2$.

Recent developments have opened the possibility of extending their use in relatively high energy sampling calorimetry, based on the idea of measuring total streamer charges, which is the equivalent of counting sampled tracks with a spatial grain of the order of 0.1 cm^3.

This paper will review the basic features and technology of the Mont Blanc PST's, together with their applications and developments.

The resistive cathode method can find applications in many other device configurations, and in different operation modes, which have only just been exploited [13].

The same is true for the streamer mode: for instance its application in drift chamber systems has been developed in Dubna (see the review in ref. 15).

2. Plastic streamer tubes

2.1. Structure of the device

The schematic structure of one plastic tube layer of the Mont Blanc detector, with two-dimensional readout by x and y external pick-up strips, is shown in fig. 1 [12,13].

The effective PST structure is visible in figs. 2–4. The basic element is an 8-cell (9×9 mm^2) open profile (fig. 2), made out of 1 mm thick extruded PVC, which is coated with graphite, with a minimum resistivity of 50 kΩ/square. The anode wires (silvered Be–Cu, 100 μm thick) are stretched along the open cells, being fixed in a central position every half meter by plastic spacers, and soldered at both ends on two printed circuit boards.

The use of plastic spacers, necessary in any case to avoid electromechanical instabilities, is also in practice essential because they allow the operation of very long tubes without strict planarity requirements.

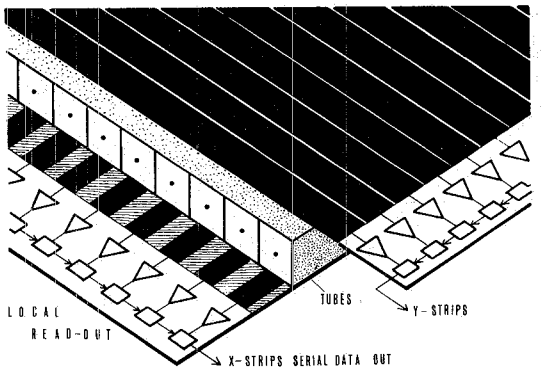

Fig. 1. Schematic structure of one PST layer of the Mont Blanc detector.

The 8-tube structure is closed by a PVC cover sheet (0.5 mm thick), placed on top of the open profile. The cover sheet is coated with graphite, with a minimum resistivity of 200 kΩ/square.

Two 8-tube elements are inserted in a bi-tube container (also extruded PVC), closed by PVC end-caps. The gas, wire and cathode connections are only on one end-cap and are visible in fig. 3, which shows two 16-tube modules, 3.6 m long.

In fig. 4 one tube module is shown, together with the x and y pick-up strip elements, and one 32-channel readout card. One strip element consists of 16 aluminum strips, 40 μm thick, attached on a 1 mm thick PVC

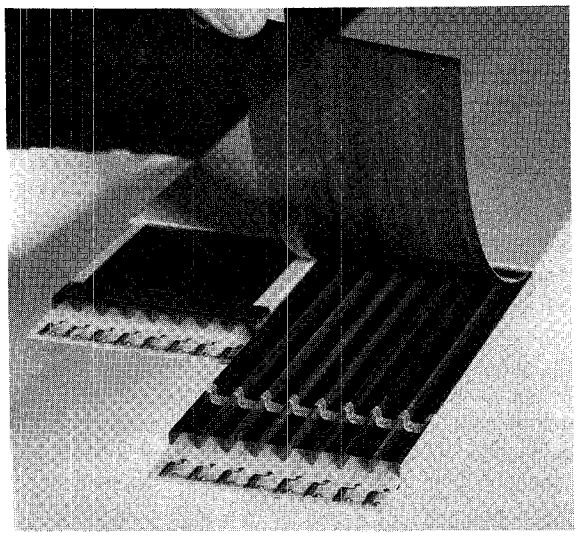

Fig. 2. Detail of the plastic streamer tubes of the Mont Blanc detector.

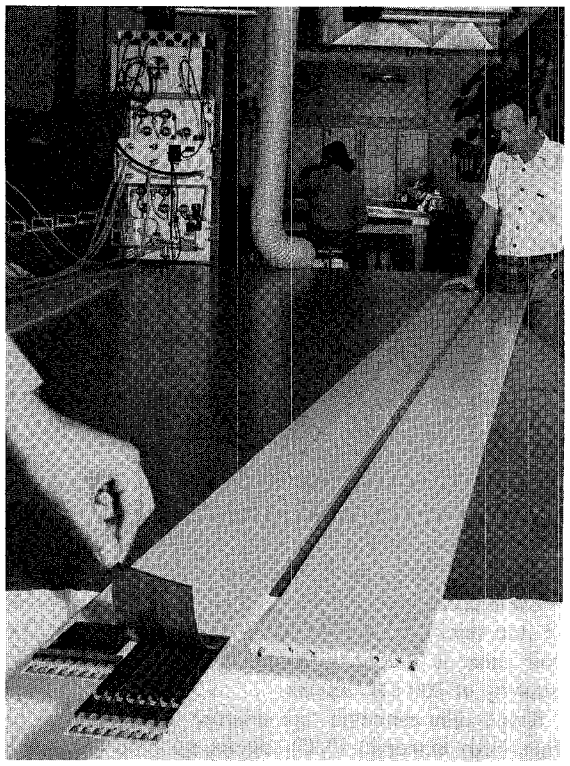

Fig. 3. Two tube modules.

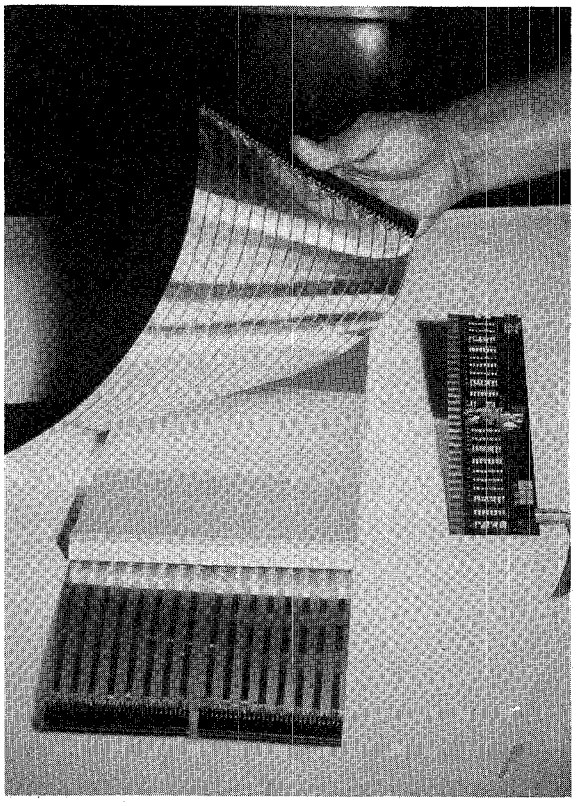

Fig. 4. Tube module, x and y strips, and readout card.

sheet, with an aluminum ground sheet on the other face and a standard connector at one end, to which a readout card is directly connected. The x-strips have a pitch of 10 mm and are 4 mm wide, in order to maximize the central-to-side-strip ratio. The y-strips are 10 mm wide and have a 12 mm pitch.

The use of strips orthogonal to the tubes to read out the second coordinate, is an example of a readout configuration uniquely allowed by the resistive cathode method. On the other hand, the use of strips in place of the direct wire readout is an example of where the same method allows a simplification of the system. Actually the simple structure of the device mainly comes from the full separation between the live part of the device (the wire-tube system, with its gas and hv connections) and the readout which is connected to the passive external pick-ups, avoiding hv insulation problems.

2.2. Streamer operation

One of the specific features of streamer tubes, beyond the large signals, is a noiseless and wide hv efficiency plateau which they can easily exhibit in a wide range of wire diameters (40–220 μm) and tube diameters (from several centimeters down to a few millimeters) [9,16].

In fig. 5 the typical singles counting rate curve as a function of the hv is shown, as obtained from wires, with an argon + isobutane (1 + 3) mixture, and due to cosmic rays and local radioactivity.

The initial rise is due to the gradual transition from proportional to streamer operation. Due to the wide pulse height gap between the two modes, the rise is widely independent of the discriminator threshold, around 0.5 mA.

The flat region corresponds to a fully efficient

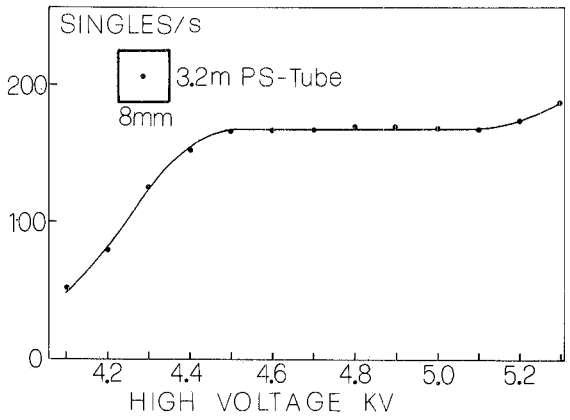

Fig. 5. Typical singles counting rate vs hv for a $0.8 \times 0.8 \times 320$ cm^3 tube with 100 μm wire, argon + isobutane (1 + 3). The wire is connected to a discriminator with 30 mV/50 Ω threshold.

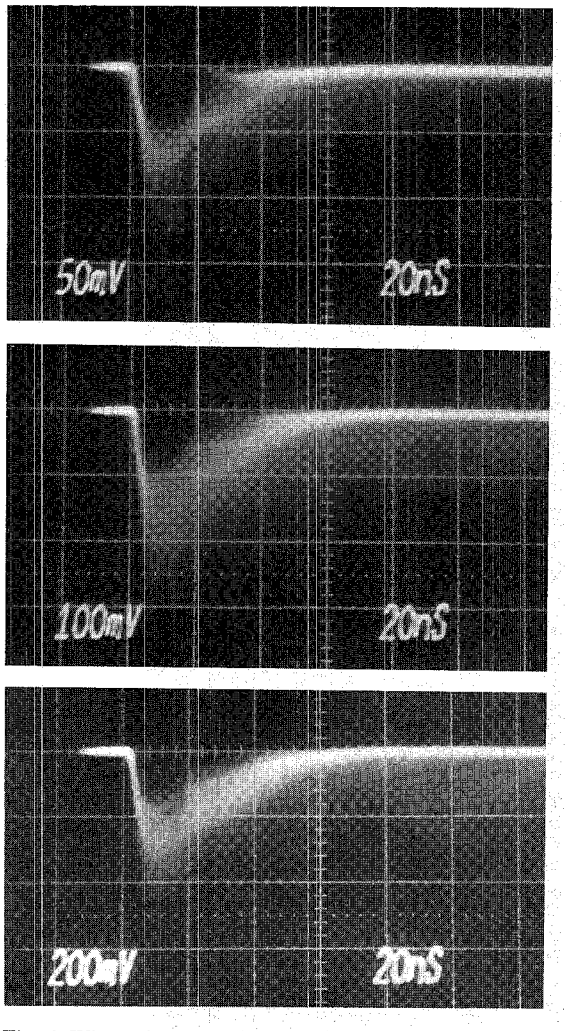

Fig. 6. Wire pulses on 50 Ω load from the tube in fig. 5, with the hv at (a) 4.5, (b) 4.85, and (c) 5.2 kV.

streamer generation, without spurious pulses. The pictures in fig. 6 show the wire pulses, directly on 50 Ω, generated by an uncollimated ^{90}Sr source, at three different hv values in the plateau region, with a maximum difference of 700 V: the pulse shape does not change, while the pulse height changes by about a factor of 4.

The rise at higher voltages of the singles rate curve is still due to streamer pulses, the generation of which is induced by the primary streamers: in fact they occur with a time correlation between them, with a delay of the order of 10^{-4} s, which suggests that they are induced by ion feedback. In practice this means that a plateau curve of the type shown in fig. 5 is typically obtained, which does not change when the ambient ionizing particle rate is changed in a very wide range: from 10^{-3} /s · cm^2 to above 10^2 /s · cm^2.

Fig. 7 shows the typical charge distribution of the wire signals, as generated by an uncollimated ^{90}Sr source, which, due to the interleaved material thickness, provides practically isotropic tracks with a wide ionizing power spectrum, down to the minimum. The granular structure of the streamer process is visible, the single and double streamer peaks being clearly resolved. Multi-streamers are essentially produced by tracks at an angle (see sect. 4), although big clusters of ionization, such as those generated by the X-rays of ^{55}Fe, can produce double streamers at an operation hv rather high in the plateau. In this respect one has to specify that the streamer mode is a substantially, but not strictly, saturated mode, like for instance the Geiger mode.

The plateau efficiency of a single tube layer, with 1×1 cm^2 tubes and 1 mm separation walls, is around 97%, as measured with minimum ionizing cosmic rays. Taking into account their angular distribution, this efficiency is obtained in a calculation where a minimum detectable track length around 1 mm is assumed.

The large amount of ionic charge developed in the streamer process introduces a large dead time, but only along a few millimeters of wire, depending on the operation parameters. From various observations one can infer that streamer tubes can be operated at rates as high as 10^2 /s · cm^2, with a few percent loss in detection efficiency due to dead time effects.

Concerning the streamer development, a possible essential picture is the following. The stages of ionization, drift and proportional amplification in proximity of the wire are the usual ones. Now the high field produces a large amplification. The correspondingly large ion space charge produces a local field of the order of the external field, and reinforces it, pointing to the

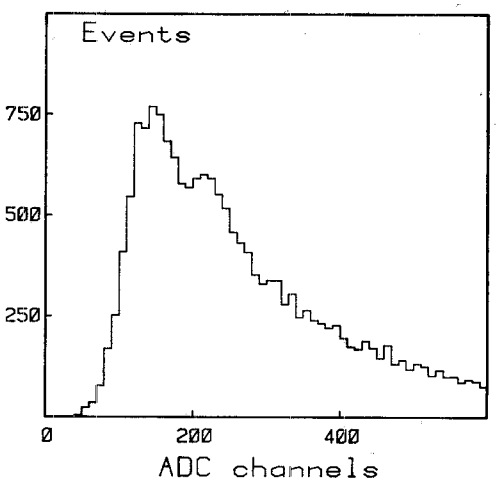

Fig. 7. Wire pulse height spectrum at the beginning of the streamer plateau, with an uncollimated ^{90}Sr source. The single streamer peak is at 30 pC.

cathode. From the simple observation that the streamers in a tube fire on the track side with repect to the wire, one can infer that the space charge distribution is largely asymmetric around the wire and has a maximum roughly corresponding to the point of arrival of the first electrons. The space charge field plus the external field act on electrons produced by photoionization and induce new avalanches to develop. In an iterative sequence, the amplification process develops towards the cathode and extinguishes itself with the proper gas mixture. The final result is a filament of ions and electrons. The latter drift to the wire giving rise to the observed current signal, which therefore is an electron signal.

2.3. Gas mixture

In order to obtain stable, uncritical, and noiseless streamer operation, with typical performances of the type discussed above, a sufficiently quenching gas mixture is needed. However, the crucial point in practice is that the minimum quenching power needed is a function of the tube dimensions: the smaller the tube, the higher must be the quenching action. Taking into account that the streamer propagates from the wire toward the cathode, the explanation for this is simple: the smaller the tube the shorter must be the streamer. In other words, in contrast to other operation modes, here the relevant gap is not the wire–cathode gap, but that left between the streamer tip and the cathode, which is fixed by the quenching action of the gas mixture.

The practical consequence is that the useful set of gas mixtures and their quenching proportions is a small subset of those useful for proportional operation [17]. The diagram in fig. 8 is a very qualitative sketch which gives the useful gas mixtures for various tube dimensions. It concerns the simple case of two-component gas mixtures between argon and a set of quenchers commonly used, in wide proportion ranges, for proportional operation.

In practice, for small streamer tubes one is substantially left only with isobutane, with which undesired effects were never observed. In particular the well known long term degeneracy effects were checked for. With 1 cm^2 tubes, either aluminum or graphite cathodes, 100 μm wires, and argon + isobutane (1 + 3), no effect was observed after having an integrated dose of $\sim 3 \times 10^9$ particles, corresponding to ~ 3 C totally integrated charge, over 1 cm tube length.

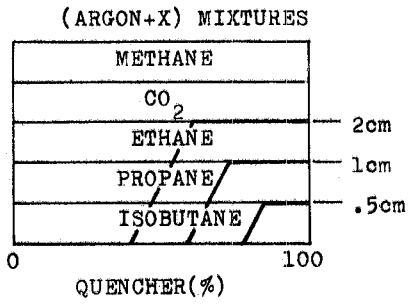

Fig. 8. Schematic diagram of useful two-component gas mixtures for various streamer tube dimensions.

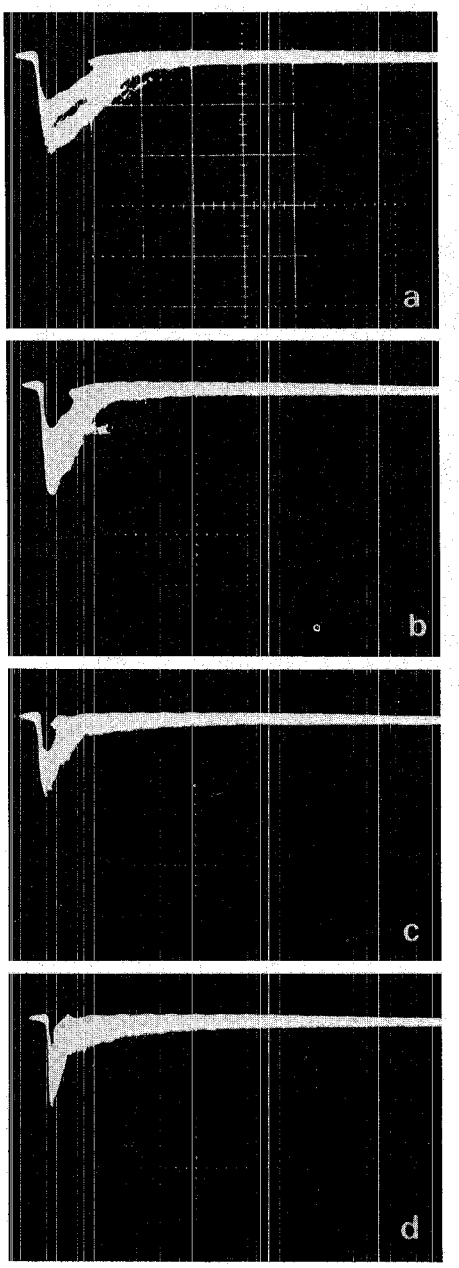

Fig. 9. Wire pulses for various isobutane concentrations in the mixture with argon: (a) 50%, (b) 60%, (c) 70%, (d) 80%. The tube is 8×8 mm^2, the wire 40 μm thick. Scale: 50 mV/div. vertical.

The pictures in fig. 9 show the streamer pulses from a 40 μm wire, when the isobutane fraction is increased from 50% to 80% in the argon + isobutane mixture. All pictures are taken with the hv set to corresponding points in the singles rate plateau curve (just above the knee). The phenomenology is very simple: only the pulse decay time changes becoming progressively shorter. The 100 μm wire gives the same behaviour: the only difference being a pulse duration about twice as long. In the Mont Blanc detector, to avoid the use of an explosive gas, the three-component gas mixture argon + CO_2 + n-pentane (1 + 2 + 1) is used, which is equivalent to the argon + isobutane (1 + 3).

2.4. Cathode material

If the gas mixture is not sufficiently quenching, UV photons emitted from the tip of the streamer can extract electrons from the cathode, which drift to the wire and trigger a new streamer just outside the dead region of the primary streamer. These secondary streamers appear as delayed pulses (afterpulses), at a constant delay time coincident with the electron drift over the cathode–wire distance. The process can be iterative and trains of afterpulses can be observed by decreasing the quencher fraction in the gas mixture, or by increasing the hv.

Due to this mechanism, the cathode material also has an influence on the choice of the gas mixture for a given tube geometry [17]. In comparing a graphite cathode with an aluminum cathode, it turns out that the latter requires a higher UV absorption by the gas mixture to suppress afterpulse generation. Fig. 10 shows the plateau curves and pulse pictures from two identical test tubes, except for the cathode material: with the same gas and hv at the beginning of the streamer plateau, the aluminum tube shows a heavy afterpulse generation, which is absent in the graphite case.

The different behaviour of graphite and aluminum is

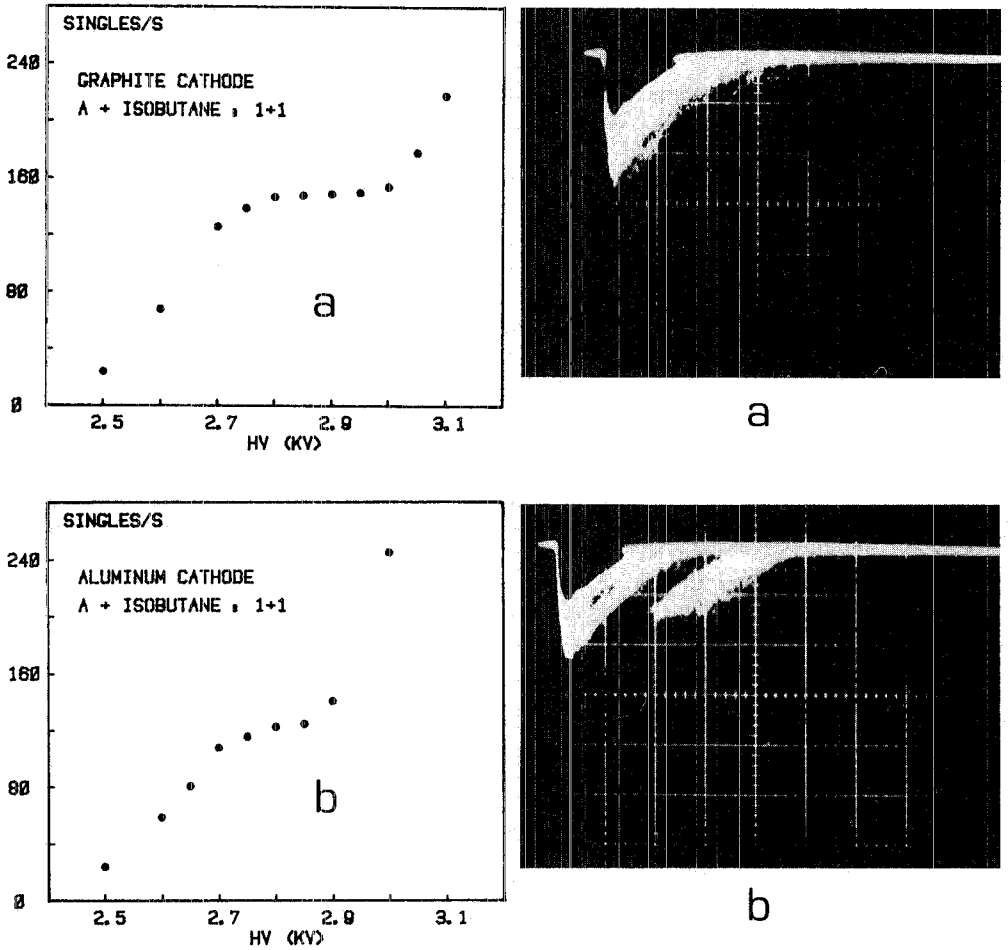

Fig. 10. Singles rate plateau curves and wire pulses for two model tubes (8×8 mm^2, 40 μm wire) different only for the cathode material.

in agreement with the fact that the work function of the former material is higher.

The graphite coated PVC surface does not create problems concerning gas purity: a 1 cm^2 tube was sealed, filled with the argon + isobutane mixture, and kept in continuous operation, inside the streamer plateau, for 2.3 months, without observing any change in tube performance.

2.5. Pick-up strips

The large signals available in the streamer mode allow the operation of strips as terminated transmission lines [13]. The 4 mm wide x-strips, with the 1 mm PVC dielectric gap connected to ground, exhibit a 50 Ω characteristic impedance and 6 ns/m characteristic propagation time. The attenuation length of such strip-lines for induced streamer pulses is above 20 m, including the dissipative effect of the adjacent resistive cathode layer. Fig. 11 shows the streamer induced signals on a 1 cm wide and 6 m long y-strip: the direct signals are visible together with the reflected signals after 12 m propagation. The strip-line faces a 100 kΩ/square resistive cathode layer.

The wire–ground line exhibits a large attenuation length of the order of 20 m due to the high characteristic impedance ($\sim$ 300 Ω), the large wire diameter and the highly conductive materials which can be used (100 μm thick silvered Be–Cu).

One can therefore arrange large layers (above 100 m^2) covered by PST's and x–y strips, with signals in the range of several mV over 50 Ω.

Concerning the operation of strips parallel to the wires, rather unexpected propagation phenomena take place, as often seen with complex transmission line configurations. The simple scheme of a direct local excitation of the strip–ground line, which works for strips at an angle, does not work in this case. Here the signal first propagates on the wire–strip line, and is only injected into the strip–ground line at the terminated end of the wire (see ref. 13 for more details).

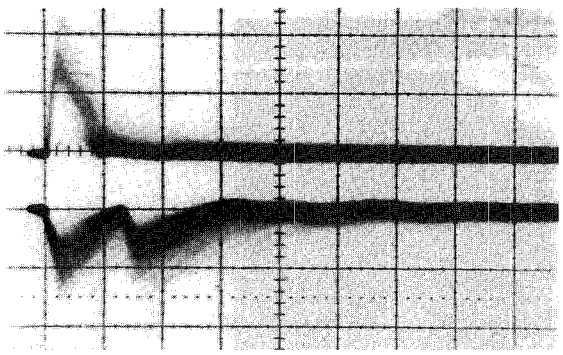

Fig. 11. Pulses from the wire and a 1 cm wide, 6 m long pick-up strip, placed outside a 8×8 mm^2 tube, with an uncollimated ^{90}Sr source placed near the readout end. The first pulse is followed by the reflected one at the open strip end (1 m propagation distance). Scale: 50 mV/div. (wire) and 10 mV/div. (strip) vertical; 20 ns/div. horizontal.

2.6. Resistive cathode transparency

The intuitive idea of pulse transmission through the resistive cathode can be simply given by saying that the resistive layer is not a shield for fast transients, which can be picked up by external electrodes.

For any given geometry and operation of wires, cathodes and pick-ups, there exists a minimum resistivity above which induced pulses are picked up, with negligible effect due to the interposed cathode, and in particular independently of its resistivity, provided it is above the minimum: in other words a transparency plateau is found, in terms of undistorted pulse transmission, as a function of cathode resistivity. The relevant fact is that in practice a useful portion of that plateau usually exists without rate limitation effects, extending over one or more orders of magnitude of the resistivity.

A detailed quantitative description of pulse shapes as a function of resistivity, also below the minimum for transparency and for a real geometry, is in general extremely complicated: calculations have been performed only for simple geometries to check the basic features [18]. To check the operation of a given configuration, in practice it is much simpler to test it, because the process is local and small model systems suffice.

The minimum resistivity for transparency varies in a wide range as a function of many parameters: in the practical cases which were examined it varied from 1 kΩ to 1 MΩ per square.

Let me qualitatively point out the basic facts and the essential parameters [18].

The high resistivity slows down the shielding action, in combination with the distributed cathode to ground capacitance. This means that the cathode to pick-up dielectric gap is of relevance: actually the cathode effect depends only on the RC product of its distributed resistivity and capacitance. For the same reasons also the pick-up electrode dimensions are of relevance: larger electrodes allow the use of smaller resistivity values. A clear role is played by the pulse duration itself: shorter pulses allow lower resistivities. In this respect one point is very important: if charge is collected the time of relevance is not the pulse duration but the integration time; if that is made arbitrarily long, the integral becomes vanishingly small, because the resistive cathode is eventually a shield.

The pictures in fig. 12 show the (negative) wire pulse and the induced pulses on two adjacent strips when a ^{90}Sr source is placed in a central position with respect to one of the strips. They refer to a cathode resistivity

respectively inside and below the transparency plateau. In the first case the strip signals reproduce, but for the sign, the wire pulse shape and are in a ratio corresponding to their position with respect to the streamer position. In the second case, the pulse shape distortion on the central strip has an obvious shape: it is simply differentiated, corresponding to the induced charge build-up on the resistive cathode. The pulse shape on the side strip has a less obvious shape: it rises higher at first, before being eventually differentiated. This is due to the shielding mechanism of the cathode, where, at this stage, the negative charge accumulated on the central region implies a positive charge distribution over the sides. In practice this means that when the resistivity is below the minimum for transparency, the induced charge distribution over the pick-ups appears broader, but still with an overall constant integral. Therefore the loss is in spatial accuracy and not in charge measurement, which means that the minimum resistivity is not a critical parameter.

The preceding considerations can be applied as well to pick-up pads or delay lines, although in the latter case the delay line parameters play a role [1].

A very high resistivity can impose a limitation on the maximum tolerable rate. However, in general, cathode resistivity is usually not the limiting factor [18].

Also the dissipative effects that the resistive cathode introduces in signal transmission over long pick-up elements are usually not relevant [18].

2.7. Construction technology

The PST device already described features a noticeable construction simplicity, also due to the high level of automation which can be easily introduced in the construction process [19]. This possibility basically relies on the following two aspects. The device has a high degree of modularity, consisting of substantially unidimensional elements (multi-tube and multi-strip modules), which are particularly suited to instal linear production chains. Extensive use is made of thermoplastic materials and of their specific technology, like thermo-shaping, thermo-bonding, and so on.

The graphite coating is also automated, using a device essentially based on the operation principle of the felt pen and using a commercial conductive varnish [13]. A graphite coating is obtained, with extremely good mechanical and chemical resistance.

Before this graphite coating method was developed, a systematic search on the possibility of using carbon-doped conductive plastics was made [9]. A few commercial types were tested, and two negative features were found, which induced us to give up the attempt: (1) in general a conductive plastic of that type does not work when used as a cathode in a wire device operated in a high current mode like the streamer (self-sustaining discharges take place); (2) it is much more difficult to control resistivity in comparison with a surface coating.

2.8. Electrodeless tubes

Making use of the electrodeless drift chamber idea, a simplified PST version has been tested [20]. The tubes seem to work as well if the top cover sheet visible in fig. 2 is not mounted. In this case the field on the top side is shaped by the positive charge accumulated on the plastic container (fig. 13). Two standard tube modules of

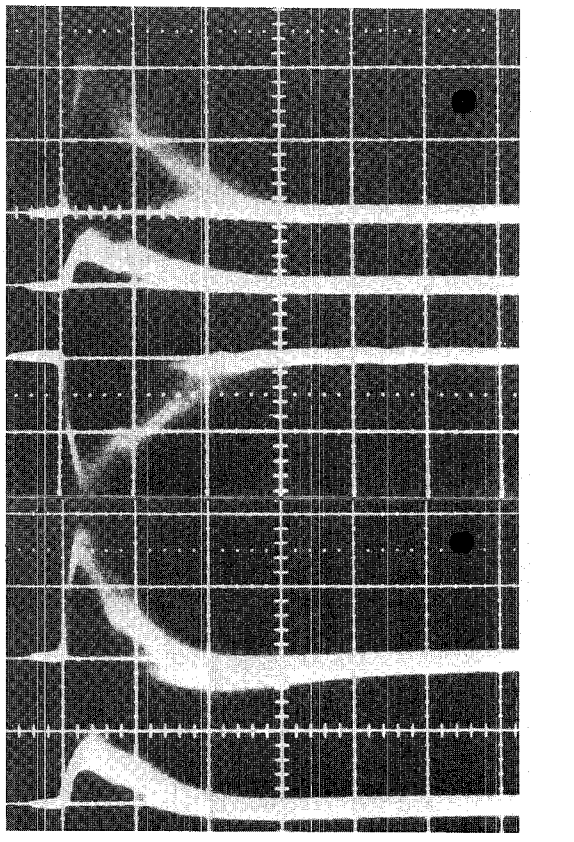

Fig. 12. Pulse from the central, side strip and wire for a cathode resistivity inside the transparency plateau (top picture) and at about 1/4 the knee value (bottom picture). Strip and wire are terminated by 50 Ω. Scale: 50 mV/div. (wire), 10 mV/div. (strip) vertical; 20 ns/div. horizontal.

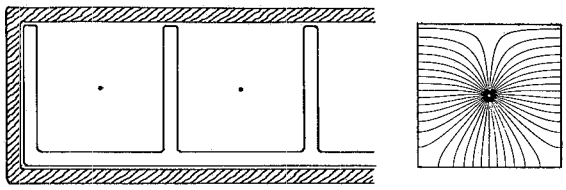

Fig. 13. Electrodeless PST's: schematic and calculated structure.

the Mont Blanc detector have been substituted with two coverless modules, to perform a long term test. The only negative feature of the electrodeless device seems to be the lack of freedom for frequent changes of the hv operation point. Also it is worth mentioning that in this case it is impossible to ground the wires and to connect the graphite to a negative hv. However, the large simplification in construction seems to largely compensate for these aspects.

3. Digital strip readout

The Mont Blanc proton decay detector is a digital tracking calorimeter. One event (a quasi-elastic neutrino interaction) is shown in fig. 14 [14]. The two views are given by the x–y strip patterns on two faces of a cube of 3.5 m side. The strips are connected to a local digital (YES/NO) readout with a threshold around 5 mV/50 Ω. Average strip multiplicity for normal track incidence is $x = 1.1$, $y = 1.6$. The low noise of streamer tubes is particularly suited to this kind of experiment, ensuring soft triggering and clean patterns. The singles counting rate for the single tube, not near to the side walls, is 0.8/s and is due to the radioactivity of the detector material. The clean singles counting also allows simple monitoring of the detector: cosmic rays are useless on the short term, due to their very low rate, around 1/10 days × tube. However, actually the most direct control of the detector status is the total tube current readout, which is a few μA.

The PST device specifically developed for this experiment, due to its high degree of modularity, can fit into many different experimental lay-outs in different applications.

The independent modularity of tubes and pick-ups and their adjustable length allow them to be assembled together to cover almost continuously a wide range of surface dimensions. Due to the flexibility that the pick-ups can have (see the strips in fig. 4), they can be adapted also to cylindrical configurations.

The drawing in fig. 15 shows one cosmic ray event from the experiment on neutron–antineutron oscillation at the Grenoble nuclear reactor [21]. Here the PST's are also used in a digital tracking calorimeter arrangement. This experimental situation shows the possibility of using PST's in a non-negligible background environment, due to soft photons in this case, generating a singles rate of $\sim 2 \times 10^4$ /m^2 × s.

Other PST detectors have been built for use: (1) in digital electromagnetic calorimeters, in the 1 GeV shower region (the APPLE experiment at LEAR and the experiment R422 at ISR) [22]; (2) in tracking calorimeters to study $p\bar{p}$–$n\bar{n}$, again at LEAR; (3) in the cylindrical shower pre-sampler in front of the JADE lead–glass system (which is also the basic design of the OPAL-LEP electromagnetic calorimeter).

The 1 cm strips and the simple digital readout give a spatial accuracy of ~ 3 mm (equivalent σ). Simple hit counting in shower patterns, which is equivalent to counting sampled tracks, gives the shower energy with a resolution similar to that obtainable with scintillation counters, as pointed out a few years ago in connection with flash chamber development [23]. This method is limited to low energy calorimetry (around 1 GeV for electromagnetic showers and depending also on detector

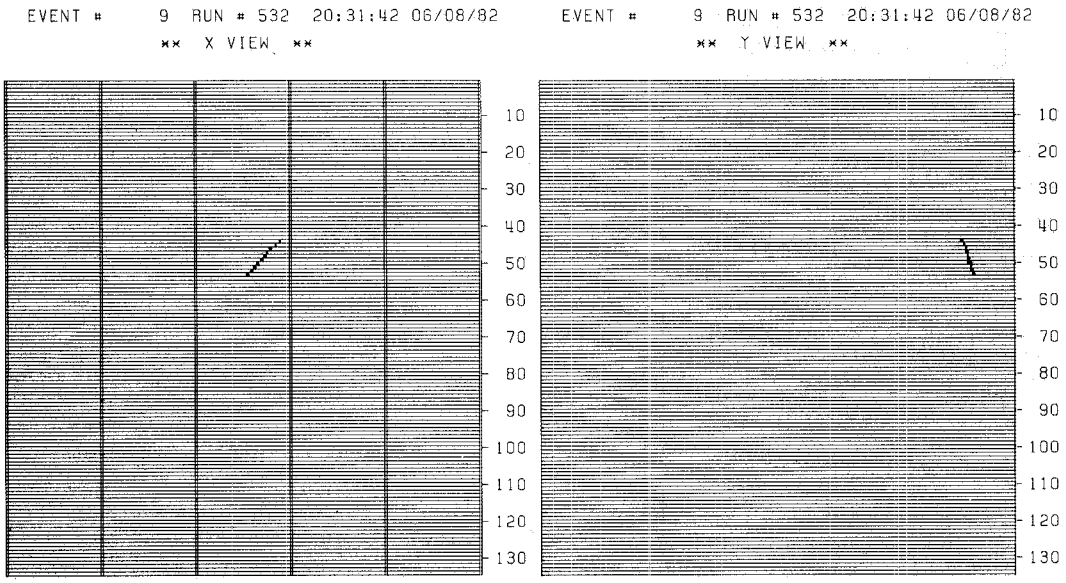

Fig. 14. A neutrino interaction in the Mont Blanc detector.

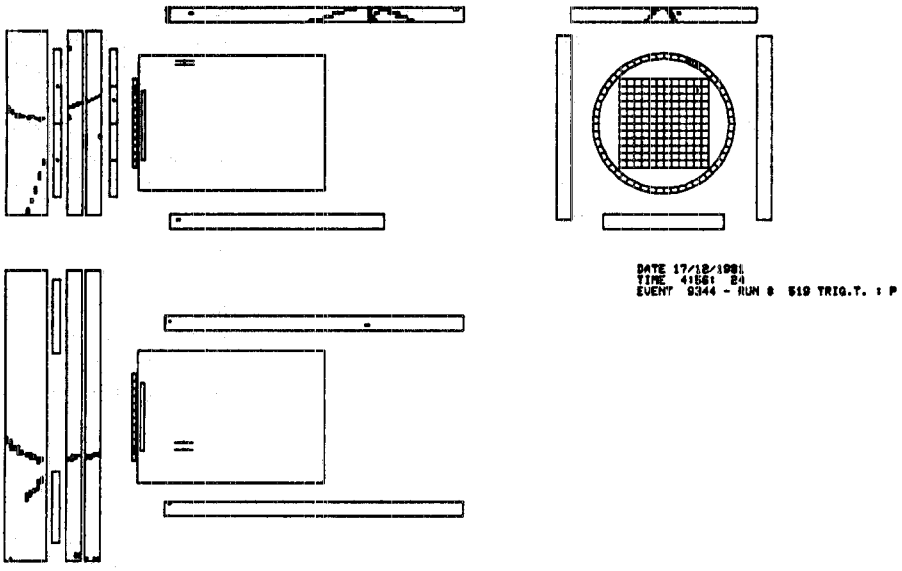

Fig. 15. Cosmic ray event in the n–$\bar{n}$ oscillation experiment at Grenoble.

density) where the track density is so low as to give a negligible occurrence of more than one track in the same tube element [24].

4. Streamer charge readout

4.1. Charge readout

A PST system with charge readout over the y-strips has been proposed to be implemented in the μ identifier of UA1 [25]: the determination of the charge centroid is expected to give a spatial accuracy around 0.5 mm. The large induced signals available (several pC) allow the design of a simple capacitive storage and multiplexing circuitry.

Streamer charge readout also opens the possibility of using PST in relatively high energy calorimetry. The use of a localized and saturated mode device with charge readout in sampling calorimeters has been introduced in the PEP-4 electromagnetic calorimeter, with wire chambers operated in a (true) limited Geiger mode [26]. The basic idea here is that the total charge measures the total number of elementary discharges (limited Geiger or streamer), which is equivalent to counting sampled tracks and therefore to measure shower energy. The basic advantages in this approach, over proportional wire calorimeters, would be: improved signal/noise ratio, simpler monitoring, and improved energy resolution, due to the absence of the Landau tail. Actually one would expect to achieve an energy resolution near to that of plastic scintillator calorimeters. As with hit counting calorimeters, but at much higher shower energies, a system of this type will exhibit a deviation from linearity in the charge–energy response and a deviation from the $1/\sqrt{E}$ behaviour of the fractional energy resolution, due to track counting losses coming from multihits in the same saturated wire region.

The structure of the PST device allows the arrangement of the calorimeters with both projective (strips or delay lines) and oriented tower structures (by simple pad wiring). This simultaneously allows high spatial accuracy and unambiguous shower localization in space to be obtained.

A number of PST test calorimeters have been built and tested, both for electromagnetic and hadron showers, within different LEP groups.

All these tests have made use of the same PSTs, with different pick-up arrangements: a further direct demonstration of their flexibility of use.

4.2. Electromagnetic calorimeters

Fig. 16 shows the total streamer charge (from wires) as a function of electron energy, and the energy resolution, for an electromagnetic test calorimeter with the following relevant parameters [27]: tube active cross section: 9×6 mm^2; 60 μm wires; argon + isobutane: 1 + 5; sampling: 2 mm lead; 20 r.l. total depth; average r.l.: 3.3 cm. The tubes were operated just at the beginning of the efficiency plateau, with a single streamer charge signal of 7 pC. The linear energy range turns out to be relatively wide: 10% non-linearity at 25 GeV. It turns out to be about twice as wide with respect to that obtained in a preceding test with standard PSTs [28]: 9×9 mm^2 tubes, 100 μm wire, argon + isobutane: 1 + 3.

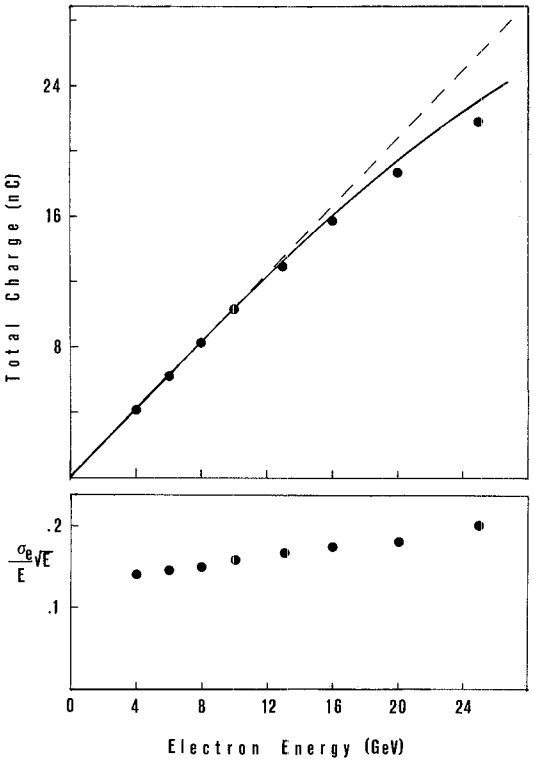

Fig. 16. Total streamer charge from wires and energy resolution as a function of electron energy.

The comparison of the results in fig. 16 with the limited Geiger results allows an estimate of the streamer obscuration length of around 1 mm (the length of the dead wire region due to a single streamer).

As far as the energy resolution is concerned, the best value occurs at the lowest energy point (4 GeV), where it is 7%. This value appears to be about 20% better than that obtainable in the proportional mode, but it is still rather higher than the plastic scintillator case. Taking into account the Monte Carlo study of the Geiger calorimeter in ref. 26, this is probably related to unavoidable track counting losses at the dense electromagnetic shower core even in the linear range; furthermore, the simple image of counting tracks by counting streamers is only approximate. Single tracks at an angle can fire more than one streamer, so that soft track obliquity fluctuations play a role.

The 1 mm streamer obscuration length estimated from the non-linearity in the response, when compared to the 6 mm gap, would indicate a large overestimate for the inclined track lengths. Actually the streamer obscuration length measured from pulse heights, due to inclined tracks in a tube, was 3 mm. A possible solution to this apparent contradiction is the following: the space charge of a streamer will introduce a smooth depression in the electric field distribution along the wire, so that the next firing streamer will occur at a distance which is a function of the available ionization density and distribution, which will also affect the streamer pulse height. The shape of the pulse height distribution of fig. 7 confirms this argument: the double streamer peak is at less than twice the single streamer peak amplitude.

Concerning angle effects only, a measurement with the electron beam at 30° with respect to the normal incidence, giving tracks inclined along the wires, shows a good overall angular behaviour: no change in the charge response, and a deterioration of the energy resolution exactly according to the increased effective sampling thickness.

4.3. Hadron calorimeters

A hadron test calorimeter has been built using standard PSTs, and having the following relevant parameters [29]: 9×9 mm^2 tube cross section, 100 μm wires, argon + isobutane: 1 + 3; 4 cm iron sampling; 1 m of iron total depth; average density: 70% of iron density.

Tubes were equipped with digital x-strips on one side, and 60×60 cm^2 pads on the other side. The tubes were operated just at the beginning of the streamer plateau, with a 30 pC single streamer pulse height. The big charge signals allow the setting, on the very large pad capacitance, of signals in the millivolt range, which is very important for trigger purposes.

The single tube response to single tracks, at various angles with respect to normal incidence, in a plane containing the wire, is shown in fig. 17. A streamer obscuration length of 4.5 mm is estimated here. In identical tube operation conditions, the streamer obscuration length estimated from the non-linearity in an electromagnetic test calorimeter response was 1.7 mm [28]: this result reproduces what was found with the test module discussed in sect. 4.2. The width for the streamer pulse height distribution at normal incidence (single streamer) is $\sigma = 25\%$. The single streamer peaks at 30 pC. The small tail on the right is consistent with δ-ray production in the material in front by the energetic particles (20 GeV pions).

The energy response (by total pad charge readout) and resolution is shown in fig. 18. The small non-linearity around 100 GeV could actually be due to effects of rate, which was around the maximum estimated to be tolerable when charge readout is performed: $\sim 10^5$ particles/s $\cdot$ m^2. The energy resolution in the linear range appears to be within 10% that of plastic scintillator calorimeters. The energy resolution of PSTs in hadron calorimeters appears to be relatively better than in electromagnetic calorimeters. This can be related to the basically different track patterns in the hadronic and electromagnetic cascades. The attractive feature of a

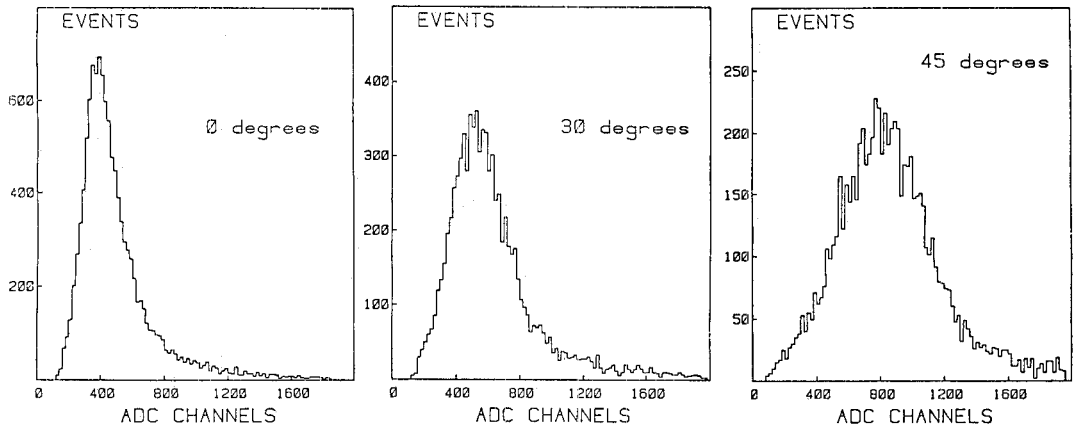

Fig. 17. Wire pulse height distribution as a function of track angle.

PST hadron calorimeter with respect to standard plastic scintillator systems is that it can simultaneously and easily give a fine grain tracking, at least in one projection, through the iron. This allows self-monitoring of the calorimeter, by comparing the charge response with the much more stable hit counting. Also this can influence the basic design of the μ identifier. On one side continuous tracking of muons through the iron looks to be itself of help in π/μ discrimination, essentially due to the fact that π shower patterns in the few 10 GeV range do not saturate the hit pattern. On the other side PSTs with x–y strips can be used in the outer layers, so providing an integrated and homogeneous hadron–muon detector [30].

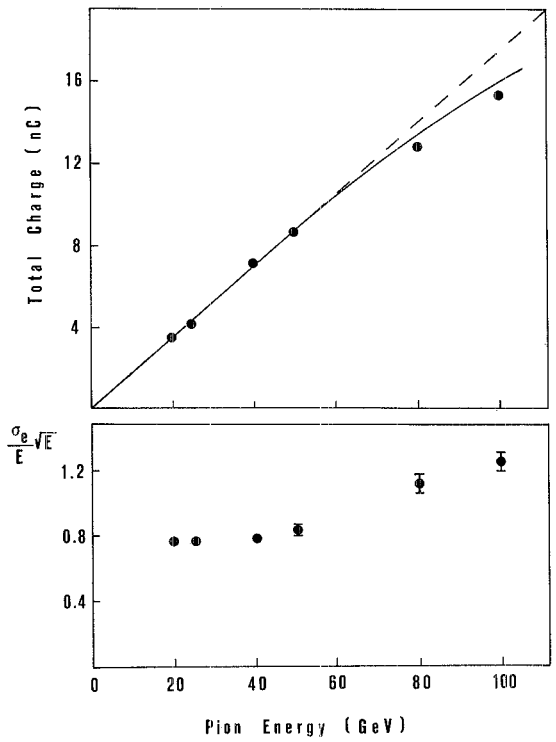

Fig. 18. Total streamer charge from pads and energy resolution as a function of pion energy.

5. Conclusions

The work on streamer charge readout calorimeters is only at its beginning, concerning both tests and Monte Carlo simulations. For instance, the insufficient knowledge of streamer response to clusters of tracks does not allow straightforward Monte Carlo simulation of detectors. Anyway, by acting on obvious parameters such as tube dimensions and gas mixture, as already shown, one can envisage that the performance in detecting high energy showers can be further improved. With 5×5 mm^2 tubes one can approximately extrapolate a 50 GeV linear range for electromagnetic lead sampling calorimeters and 500 GeV for hadron iron sampling calorimeters.

PSTs, when compared at an absolute level with other detectors or combination of detectors, often do not allow the achievement of the best performance in terms of spatial accuracy, energy resolution, and so on. But very often there are experiments which intrinsically do not ask for the best performance. Even when a better performance would not be of negligible importance, other considerations may be of more relevance, like cost, reliability and the objective risk of not attaining in the real experiment the intrinsic detector performance, due to complexity and criticity of operation. In this respect the simplicity of construction and operation of PSTs, together with their flexibility in matching complex readout topologies, are points in their favour.

They have anyway one specific field of use: the very large area tracking calorimeters, due to the high

signal/noise ratio ensured by the streamer mode. Furthermore they look to be able to be developed into a flexible modular standard.

The development of plastic streamer tubes is the result of many years of work by many people, in particular G. Battistoni, P. Campana, U. Denni, G. Mazzenga, G. Nicoletti, who were involved since the early development, and P. Picchi with his group, for the more recent developments.

For the engineering development invaluable help came from the Frascati technical division (R. Bonini and his collaborators), the CERN-EF (A. Dalluge and M. Jeanrenaud), and the Milano and Torino group technicians.

I am indebted to many others for decisive encouragement, discussions, suggestions, for the more recent developments. In this respect I want to thank in particular U. Amaldi and K. Winter, and also G. Barbiellini, P. Dal Piaz, E. Fiorini, A. Minten, C. Rubbia.

References

[1] G. Battistoni et al., Nucl. Instr. and Meth. 152 (1978) 423.
[2] C. Bacci et al., Phys. Lett. 86b (1979) 234.
[3] C. Grunberg et al., Nucl. Instr. and Meth. 78 (1970) 102.
[4] S. Brehil et al., Nucl. Instr. and Meth. 123 (1975) 225.
[5] G. Charpak et al., IEEE Trans. Nucl. Sci. NS-25 (1978) 122.
[6] J. Fisher, Nucl. Instr. and Meth. 151 (1978) 451.
[7] G.D. Alekseev et al., Lett. Nuovo Cim. 25 (1979) 157.
[8] M. Atac and A.V. Tollestrup, Preprint FN-339, Fermilab (July 10, 1981).
[9] G. Battistoni et al., Nucl. Instr. and Meth. 164 (1979) 57.
[10] B. Grelaud et al., LAL-78/25 (1978).
[11] M. Jonker et al., Nucl. Instr. and Meth. 215 (1983) 361.
[12] G. Battistoni et al., Proposal for an experiment on nucleon stability, Frascati–Milano–Torino (1979).
[13] G. Battistoni et al., Nucl. Instr. and Meth. 176 (1980) 297.
[14] G. Battistoni et al., Phys. Lett. 118B (1982) 461.
[15] G.D. Alekseev et al., Fiz. Elem. Chastits At. Yadra 13 (1982) 703.
[16] G. Battistoni et al., Proc. Int. Conf. on High energy physics, EPS, Lisbon (1981) p. 1061.
[17] G. Battistoni et al, Nucl. Instr. and Meth. 217 (3) (1983), in press.
[18] G. Battistoni et al., Nucl. Instr. and Meth. 202 (1982) 459.
[19] A paper with a detailed description of the construction technology is being prepared by the Frascati–Milano–Torino–CERN collaboration.
[20] G. Battistoni et al., Nucl. Instr. and Meth. 217 (3) (1983), in press.
[21] M. Baldo Ceolin, Proc. Neutrino '82 Conf., Balatonfured.
[22] CERN/ISRC/81-27 Proposal P109.
[23] L. Federici et al., Nucl. Instr. and Meth. 151 (1978) 103.
[24] E. Iarocci, Proc. Neutrino 1982 Conf., Balatonfured.
[25] UA1 Collaboration, CERN/SPSC/82-51 (1982).
[26] A. Barbaro-Galtieri et al., Nucl. Instr. and Meth. 213 (1983) 223.
[27] G. Battistoni et al., Proc. Workshop on Gas sampling calorimetry, Fermiblab, USA (1982).
[28] G. Battistoni et al., LNF-82/16 (1982) and Proc. Int. Conf. on Instrumentation for colliding beam physics, Stanford (1982).
[29] G. Battistoni et al., Proc. Workshop on Gas sampling calorimetry, Fermilab, USA (1982).
[30] ALEPH design, by Bari–Frascati–Pisa collaboration.